

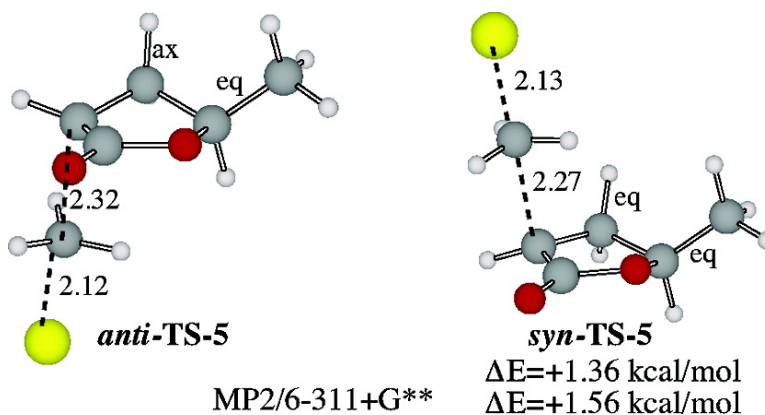
Article

## A Theoretical Study on the Origin of $\pi$ -Facial Stereoselectivity in the Alkylation of Enolates Derived from 4-Substituted $\pi$ -Butyrolactones

Kaori Ando

*J. Am. Chem. Soc.*, **2005**, 127 (11), 3964-3972 • DOI: 10.1021/ja044995n • Publication Date (Web): 25 February 2005

Downloaded from <http://pubs.acs.org> on March 24, 2009



### More About This Article

Additional resources and features associated with this article are available within the HTML version:

- Supporting Information
- Links to the 4 articles that cite this article, as of the time of this article download
- Access to high resolution figures
- Links to articles and content related to this article
- Copyright permission to reproduce figures and/or text from this article

[View the Full Text HTML](#)

## A Theoretical Study on the Origin of $\pi$ -Facial Stereoselectivity in the Alkylation of Enolates Derived from 4-Substituted $\gamma$ -Butyrolactones

Kaori Ando\*

Contribution from the College of Education, University of the Ryukyus, Nishihara-cho, Okinawa 903-0213, Japan

Received August 19, 2004; E-mail: ando@edu.u-ryukyuu.ac.jp

**Abstract:** The alkylation of 4-methoxymethyl- $\gamma$ -butyrolactone enolate with methyl chloride was studied at the B3LYP/6-31+G\* level. Conformer search of the free enolate gave 15 unique conformers within 5.39 kcal/mol. The transition structures for both anti- and syn-attacks of methyl chloride on these 15 conformers were located. In all cases, the anti-transition structures are more stable than the corresponding syn-ones. The alkylation of  $\gamma$ -valerolactone was studied at the MP2, B3LYP, and HF levels of theory with the 6-31+G\* basis set in the presence of Li<sup>+</sup> and dimethyl ether molecules. Basis set effects were also examined by the comparison of the MP2 results with the 6-31+G\*, 6-31+G\*\*, and 6-311+G\*\* basis sets in one case. This study shows that the main source of the anti-selectivity of 4-substituted  $\gamma$ -butyrolactones is eclipsing strain in the syn-transition structures.

### Introduction

The carbon–carbon bond formation via enolate alkylation continues to be an important area in organic synthesis. If the enolate contains an asymmetric center, the resultant  $\pi$ -faces of the enolate are diastereotopic, and diastereoselective introduction of substituents can be expected. Therefore, the origin of  $\pi$ -facial stereoselectivity of enolates is an important area of investigation. Houk and co-workers, including this author, have performed a theoretical study to determine the origin of stereoselectivity in the pyrrolidinone enolate (**1**) alkylations.<sup>1</sup> From ab initio calculations, we concluded that the stereochemistry of the pyrrolidinone enolate alkylations can be explained by a combination of torsional strain (eclipsing strain)<sup>2</sup> and steric effects in the transition states. For other types of stereoselective reactions, Houk et al. have reported computational support for the Felkin model,<sup>3</sup> in which stereoselectivity is controlled by torsional strain and steric interactions.<sup>4</sup> Now I would like to extend this research to the oxygen counterparts, that is,  $\gamma$ -butyrolactones **2**, which also show high anti-selectivity.

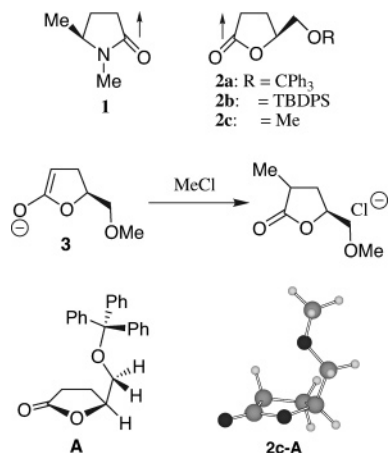
Alkylations of the enolates generated from enantiopure 4-hydroxymethyl- $\gamma$ -butyrolactone derivatives such as **2a** and **2b**, obtained from L-glutamic acid, have been used for successful syntheses of a variety of optically active compounds by the

laboratories of Koga and Tomioka,<sup>5</sup> Takano,<sup>6</sup> Hanessian,<sup>7</sup> and others.<sup>8,9a</sup> The reactions afford products with good to excellent anti-selectivity (for example, 96:4–99:1 for **2a**<sup>5c</sup>). However, the origin of  $\pi$ -facial selectivity of those enolates remains to be elucidated. From NMR analysis and MM2 force field calculations, Koga and Tomioka concluded that 4-(trityloxy)methyl- $\gamma$ -butyrolactone (**2a**) has the predominant conformer **A**, in which the (trityloxy)methyl group is located above the plane of  $\gamma$ -lactone ring.<sup>5c</sup> A similar conformation has also been determined for the  $\alpha$ -*exo*-ethylidene lactone by both X-ray crystallographic and <sup>1</sup>H NMR analyses.<sup>10</sup> They suggested that the oxygen atom in the side chain caused this conformation and speculated that the syn-attack of an electrophile would encounter

- (1) Ando, K.; Green, N. S.; Li, Y.; Houk, K. N. *J. Am. Chem. Soc.* **1999**, *121*, 5334–5335.
- (2) Hyperconjugation is reported to be the origin of torsional strain: Pophristic, V.; Goodman, L. *Nature* **2001**, *411*, 565–568.
- (3) (a) Cherest, M.; Felkin H.; Prudent, N. *Tetrahedron Lett.* **1968**, 2199–2204. (b) Cherest, M.; Felkin H. *Tetrahedron Lett.* **1968**, 2205–2208.
- (4) (a) Ando, K.; Condroski, K. R.; Houk, K. N.; Wu, Y.-D.; Ly, S. K.; Overman, L. E. *J. Org. Chem.* **1998**, *63*, 3196–3203. (b) Ando, K.; Houk, K. N.; Busch, J.; Menassé, A.; Séquin, U. *J. Org. Chem.* **1998**, *63*, 1761–1766. (c) Behnam, S. M.; Behnam, S. E.; Ando, K.; Green, N. S.; Houk, K. N. *J. Org. Chem.* **2000**, *65*, 8970–8978.

- (5) (a) Tomioka, K.; Koga, K. *Tetrahedron Lett.* **1979**, *20*, 3315–3318. (b) Tomioka, K.; Cho, Y.-S.; Sato, F.; Koga, K. *Chem. Lett.* **1981**, 1621–1624. (c) Tomioka, K.; Cho, Y.-S.; Sato, F.; Koga, K. *J. Org. Chem.* **1988**, *53*, 4094–4098.
- (6) (a) Takano, S.; Yonaga, M.; Chiba, K.; Ogasawara, K. *Tetrahedron Lett.* **1980**, *21*, 3697–3700. (b) Takano, S.; Chiba, K.; Yonaga, M.; Ogasawara, K. *J. Chem. Soc., Chem. Commun.* **1980**, 616–617. (c) Takano, S.; Kasahara, C.; Ogasawara, K. *J. Chem. Soc., Chem. Commun.* **1981**, 637–638. (d) Takano, S.; Morimoto, M.; Ogasawara, K. *J. Chem. Soc., Chem. Commun.* **1984**, 82–83. (e) Hatakeyama, S.; Numata, H.; Takano, S. *Tetrahedron Lett.* **1984**, *25*, 3617–3620.
- (7) (a) Hanessian, S.; Murray, P. J.; Sahoo, S. P. *Tetrahedron Lett.* **1985**, *26*, 5623–5626. (b) Hanessian, S.; Sahoo, S. P.; Murray, P. J. *Tetrahedron Lett.* **1985**, *26*, 5631–5634. (c) Hanessian, S.; Abad-Grillo, T.; McNaughton-Smith, G. *Tetrahedron* **1997**, *53*, 6281–6294.
- (8) (a) Robin J. P.; Gringore, O.; Brown, E. *Tetrahedron Lett.* **1980**, *21*, 2709–2712. (b) Baker, W. R.; Pratt, J. K. *Tetrahedron* **1993**, *49*, 8739–8756. (c) Dorsey, B. D.; Levin, R. B.; McDaniel, S. L.; Vacca, J. P.; Guare, J. P.; Darke, P. L.; Zugay, J. A.; Emmini, E. A.; Schleif, W. A.; Quintero, J. C.; Lin, J. H.; Chen, I.; Holloway, M. K.; Fitzgerald, P. M. D.; Axel, M. G.; Ostovic, D.; Anderson, P. S.; Huff, J. R. *J. Med. Chem.* **1994**, *37*, 3443–3451. (d) Kang, K. H.; Cha, M. Y.; Pae, A. N.; Choi, K. I.; Cho, Y. S.; Koh, H. Y.; Chung, B. Y. *Tetrahedron Lett.* **2000**, *41*, 8137–8140. (e) Marshall, J. A.; Johns, B. A. *J. Org. Chem.* **2000**, *65*, 1501–1510.
- (9) (a) Anceau, C.; Dauphin, G.; Coudert, G.; Guillaumet, G. *Bull. Soc. Chim. Fr.* **1994**, *131*, 291–303. (b) Diaz, D.; Martin, V. S. *Org. Lett.* **2000**, *2*, 335–337.
- (10) Tomioka, K.; Kawasaki, H.; Iitaka, Y.; Koga, K. *Tetrahedron Lett.* **1985**, *26*, 903–906.

a severe steric hindrance from the trityloxymethyl group, if the enolate derived from **2a** took a conformation similar to **A**. However, the conformational analysis of the enolate from **2a** has not been studied. To understand the stereoselectivity of this alkylation reaction of **2**, a computational study was performed.



Many lithium enolates have been known to exist primarily as tetrameric and dimeric aggregates in ethereal solvents.<sup>11</sup> However, Streitwieser and co-workers experimentally showed that the alkylation reaction of lithium enolates occurs via the monomeric ion pair even in the presence of a large excess of tetrameric and dimeric forms in many examples.<sup>12</sup> Therefore, only monomeric species were used as model systems, and the stereoselectivity of the alkylation with methyl chloride was explored in this study. The models in this study should be appropriate for the study on the origin of the stereoselectivity of the chiral lactones.

### Calculation Methods

All calculations were performed using the Gaussian 98 program.<sup>13</sup> Gibbs free energies are the values at  $-78\text{ }^{\circ}\text{C}$  (195.15 K) and 1.00 atm obtained from the frequency calculations unless otherwise noted. Most of the calculations were performed by the B3LYP hybrid functional<sup>14</sup> together with the 6-31+G\* basis set. Since the scale factor for B3LYP is very close to 1.0,<sup>15</sup> the thermal energy corrections are not scaled. Vibrational frequency calculations gave only one imaginary frequency for all transition structures and confirmed that those structures are

authentic transition structures. The structures of reactants and products were obtained by the optimization of the last structures on both sides of the IRC calculations.<sup>16</sup> The frequency calculations on their structures gave only harmonic frequencies and confirmed that they are minima. Some calculations were performed at the MP2/6-31+G\* and the RHF/6-31+G\* levels of theory. The Gibbs free energies include the corresponding zero-point energies scaled by 0.9135<sup>15b</sup> for the RHF/6-31+G\* results and 0.9670 (reported for MP2/6-31G\*)<sup>15b</sup> for the MP2/6-31+G\* results.

### Results and Discussion

**The Origin of the Stereoselectivity of  $\gamma$ -Alkoxyethyl- $\gamma$ -butyrolactone Enolate.** Koga and Tomioka used lithium diisopropylamide (LDA) in THF solvent for monoalkylation and LDA in THF–HMPA solvent system for dialkylation of **2a**,<sup>5</sup> both of which gave the anti-products high stereoselectivity. Since the stereoselectivity is little affected by the addition of HMPA to the enolates, the coordination sphere around the lithium unlikely has a big influence on the stereochemical outcome. Therefore, the free enolate **3** having a methoxy group instead of the trityloxy group was used as a model substrate, and the stereoselectivity of the alkylation of **3** with methyl chloride was explored. The conformer search of the free enolate **3** was performed using density functional calculations with the B3LYP hybrid functional and the 6-31+G\* basis set. Fifteen unique conformers were obtained within 5.39 kcal/mol (Figure 1). There are nine kinds of conformations of the methoxymethyl substituent. The eq and ax denote that the substituent group is either equatorial or axial, respectively. The energy values are the relative energies based on the energy of the most stable conformer **3-1eq**. It is interesting to note that there is no conformer like **A**. On the other hand, A-type conformer **2c-A** is the most stable one for the lactone **2c** (R = Me) (B3LYP/6-31+G\*). Therefore, the enolate has a conformational preference different from the one of the lactone. The structure **A** has the same substituent conformation as the conformer **3-8eq**, which is less stable than **3-1eq** by 4.51 kcal/mol. The corresponding axial conformer **3-8ax** could not be obtained.<sup>17</sup> It is assumed that the electrostatic repulsion between the enolate  $\pi$ -electrons and the oxygen lone pairs destabilizes the conformer **3-8ax**. Equatorial conformers are more stable than the corresponding axial conformers with two exceptions of conformers **3-2** and **3-5**, where the axial conformers **3-2ax** and **3-5ax** are more stable than the equatorial conformers **3-2eq** and **3-5eq** by 0.10–0.14 kcal/mol. Since axial  $\gamma$ -valerolactone enolate (Me instead of CH<sub>2</sub>OMe) is less stable than its equatorial one by 0.60 kcal/mol ( $\Delta E = 0.74$  kcal/mol), there should be side chain effect for the enolates **3-2** and **3-5**. The axial conformers **3-2ax** and **3-5ax** are stabilized compared with their equatorial ones by the electrostatic interactions between the negative side chain oxygen and the hydrogen, which are separated by a distance approximating the sum of their van der Waals radii (2.72 Å). The preference for an equatorial conformation is related to the greater stability of the anti-conformation of *n*-butane compared to that of the gauche conformation.

The transition structures **4** for both anti- and syn-attack of methyl chloride on these 15 conformers were located. Although there are 30 possible transition structures, 17 transition structures

- (11) Seebach, D. *Angew. Chem., Int. Ed. Engl.* **1988**, *27*, 1624–1654 and references therein.  
 (12) (a) Abu-Hasanayn, F.; Stratakis, M.; Streitwieser, A. *J. Org. Chem.* **1995**, *60*, 4688–4689. (b) Abbotto, A.; Streitwieser, A. *J. Am. Chem. Soc.* **1995**, *117*, 6358–6359. (c) Abu-Hasanayn, F.; Streitwieser, A. *J. Am. Chem. Soc.* **1996**, *118*, 8136–8137. (d) Abbotto, A.; Leung, S. S.-W.; Streitwieser, A.; Kilway, K. V. *J. Am. Chem. Soc.* **1998**, *120*, 10807–10813. (e) Wang, D. Z.; Kim, Y.-J.; Streitwieser, A. *J. Am. Chem. Soc.* **2000**, *122*, 10754–10760. (f) Wang, D. Z.; Streitwieser, A. *J. Org. Chem.* **2003**, *68*, 8936–8942.  
 (13) Frisch, M. J.; Trucks, G. W.; Schlegel, H. B.; Scuseria, G. E.; Robb, M. A.; Cheeseman, J. R.; Zakrzewski, V. G.; Montgomery, J. A., Jr.; Stratmann, R. E.; Burant, J. C.; Dapprich, S.; Millam, J. M.; Daniels, A. D.; Kudin, K. N.; Strain, M. C.; Farkas, O.; Tomasi, J.; Barone, V.; Cossi, M.; Cammi, R.; Mennucci, B.; Pomelli, C.; Adamo, C.; Clifford, S.; Ochterski, J.; Petersson, G. A.; Ayala, P. Y.; Cui, Q.; Morokuma, K.; Malick, D. K.; Rabuck, A. D.; Raghavachari, K.; Foresman, J. B.; Cioslowski, J.; Ortiz, J. V.; Stefanov, B. B.; Liu, G.; Liashenko, A.; Piskorz, P.; Komaromi, I.; Gomperts, R.; Martin, R. L.; Fox, D. J.; Keith, T.; Al-Laham, M. A.; Peng, C. Y.; Nanayakkara, A.; Gonzalez, C.; Challacombe, M.; Gill, P. M. W.; Johnson, B. G.; Chen, W.; Wong, M. W.; Andres, J. L.; Head-Gordon, M.; Replogle, E. S.; Pople, J. A. *Gaussian 98*, revision A.9; Gaussian, Inc.: Pittsburgh, PA, 1998.  
 (14) (a) Becke, A. D. *J. Chem. Phys.* **1993**, *98*, 5648–5652. (b) Lee, C.; Yang, W.; Parr, R. G. *Phys. Rev. B* **1988**, *37*, 785–789.  
 (15) (a) Bauschlicher, C. W., Jr.; Partridge, H. *J. Chem. Phys.* **1995**, *103*, 1788–1791. (b) Scott, A. P.; Radom, L. *J. Phys. Chem.* **1996**, *100*, 16502–16513.

- (16) (a) Gonzalez, C.; Schlegel, H. B. *J. Chem. Phys.* **1989**, *90*, 2154–2161. (b) Gonzalez, C.; Schlegel, H. B. *J. Chem. Phys.* **1990**, *94*, 5523–5527.  
 (17) Even in the presence of a lithium cation, **3-8ax** could not be obtained.

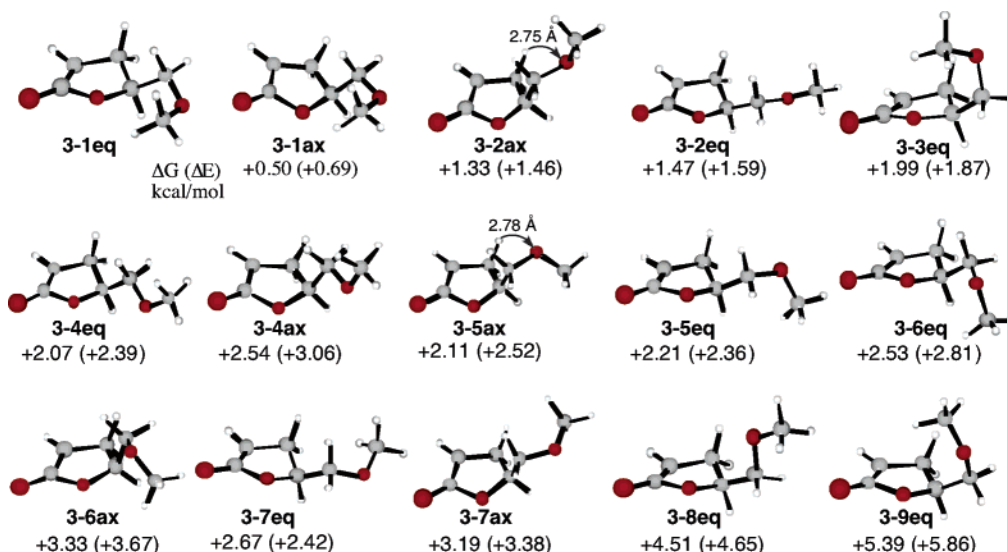


**Figure 1.** Fifteen unique conformers of the free enolate **3** and their relative Gibbs free energies at 298.15 K (kcal/mol) (B3LYP/6-31+G\*). The numbers in the parentheses are the relative energies.

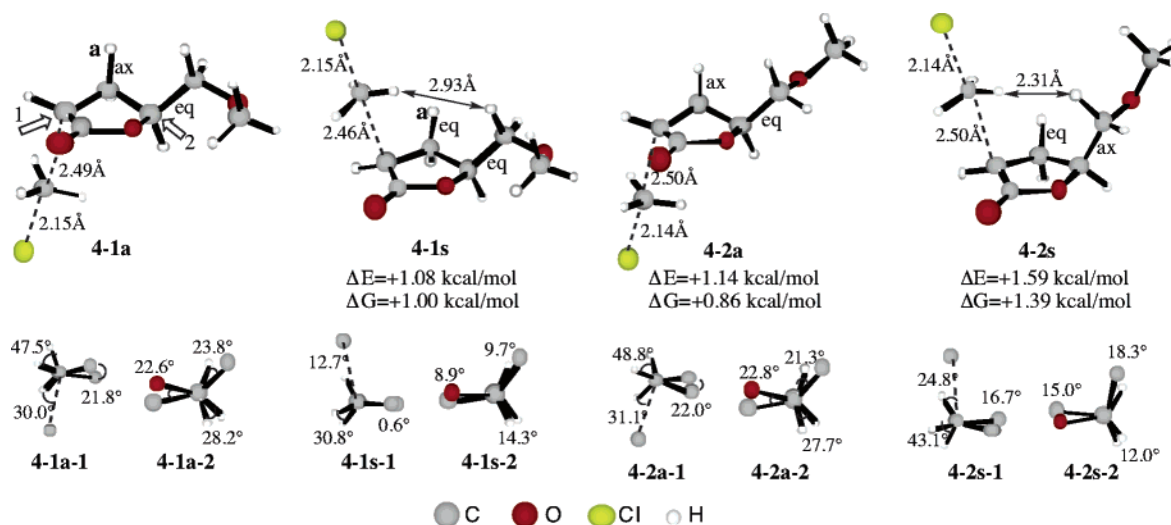


**Figure 2.** Transition structures for the anti- and syn-attacks of MeCl on **3** and their relative energies and Gibbs free energies at  $-78$  °C (B3LYP/6-31+G\*). Newman projections are viewed from the directions indicated by arrows 1 and 2 in **4-1a**.

were obtained. The equatorial and axial conformations of the side chain of **3** are exchanged during the course of optimization. In addition, a bad steric hindrance during the reaction changed the side chain conformation in the reaction of **4-9s**. The most favorable two anti-transition structures, **4-1a**, and **4-2a**, and their corresponding syn-ones are shown in Figure 2. These are derived from the enolate conformers **3-1** and **3-2**. The anti-transition structure **4-1a** is favored over the syn-transition structure **4-1s** by 1.00 kcal/mol. In these transition structures' names, the number shows the side chain conformation and "a" and "s" designate the anti- and syn-transition structure, respectively. Careful comparison of the transition structures **4-1a** and **4-1s** shows that there is no steric interaction. The distance between the incoming methyl hydrogen and the side chain hydrogen in **4-1s** is 2.93 Å, which is much longer than the sum of their van der Waals radii (2.40 Å). The Newman projections from the directions of arrows 1 and 2 are shown under their transition structures in Figure 2. They show that **4-1s** occurs with a more eclipsed arrangement. The 1.00 kcal/mol difference in energy can be compared to the 3 kcal/mol

energy difference between the staggered and the eclipsed ethane. In the anti-transition structure **4-1a**, methyl chloride approaches the lactone enolate from the axial direction with the hydrogen **a** axial and MeOCH<sub>2</sub> group equatorial. This arrangement makes **4-1a** more staggered. On the other hand, the incoming methyl chloride from the axial direction makes the hydrogen **a** equatorial in **4-1s**. Since the MeOCH<sub>2</sub> group prefers equatorial and the lactone ring becomes nearly planar, **4-1s** occurs with a more eclipsed arrangement. Similarly, the anti-transition structure **4-2a** is favored over the *syn*-**4-2s** by 0.53 kcal/mol. The Newman projections show that **4-2s** has a more eclipsed arrangement compared with the arrangement of **4-2a**. Since the enolate conformer **3-2ax** is more stable than **3-2eq**, the side chain in **4-2s** takes an axial position. Although there is a small steric repulsion between the incoming methyl group and the methoxymethyl group, the energy difference (0.53 kcal/mol) is much smaller than **4-1** because the eclipsing strain (torsional strain) is reduced in the axial methoxymethyl conformation. This implies that the electrostatic interaction between the side chain oxygen and the ring hydrogen in the lactone enolate reduces



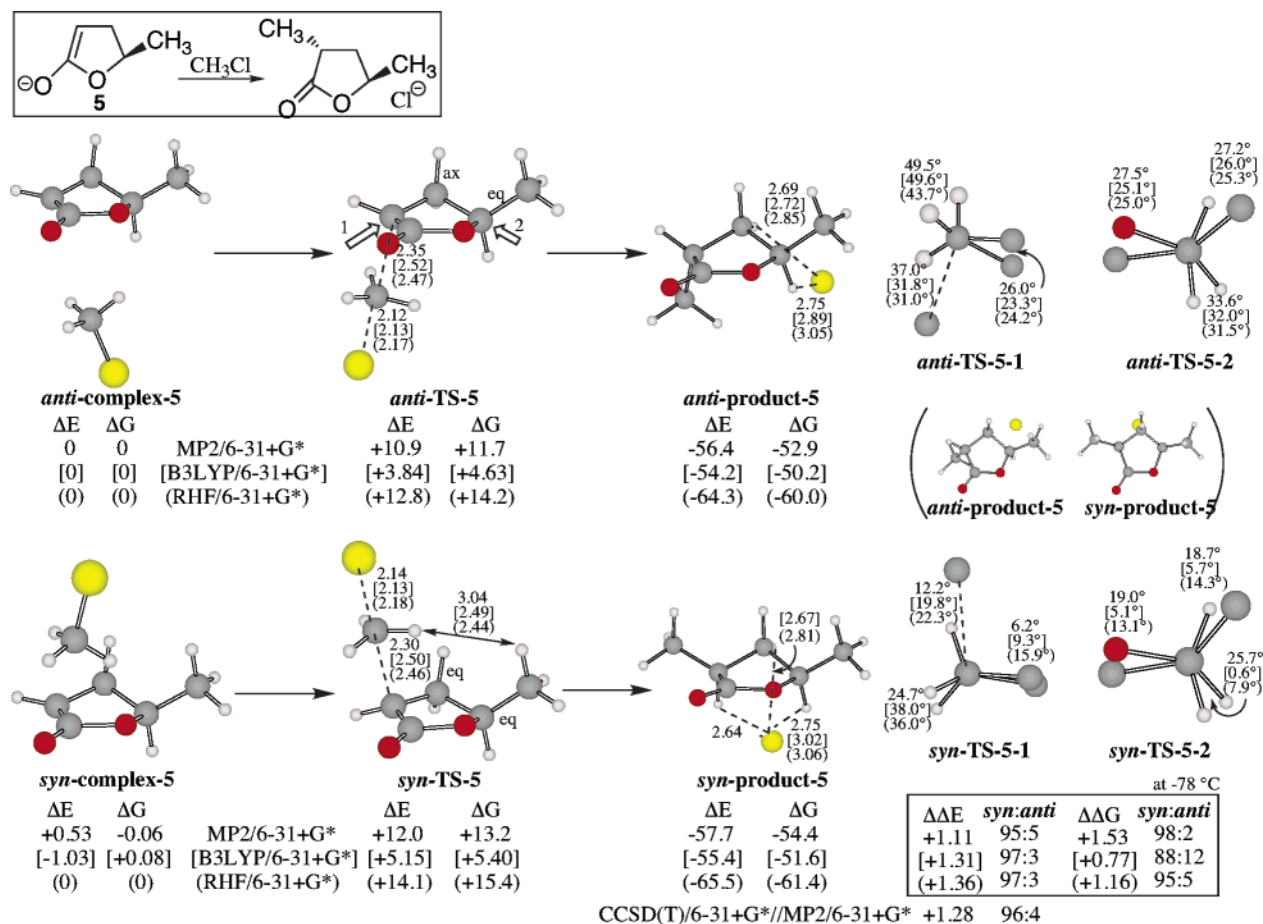


**Figure 3.** Transition structures for the anti- and syn-attacks of MeCl on the free enolate **5** (MP2/6-31+G\*).  $\Delta E$  and  $\Delta G$  are the differences in energy and the Gibbs free energy at  $-78$  °C, respectively (kcal/mol).  $\Delta\Delta E$  and  $\Delta\Delta G$  are the syn,anti-TS energy differences. The values of [B3LYP/6-31+G\*] and (RHF/6-31+G\*) levels are also shown.

the stereoselectivity. For other enolate conformers, the energy differences between anti- and syn-transition structures are 0.66–1.87 kcal/mol and all favor the anti-reaction mainly by eclipsing strain (figure in the Supporting Information). Although the most stable enolate conformer may change in the presence of a lithium cation and solvent (for the effect of these, see the latter part of this article), all the anti-transition structures are more stable than the corresponding syn-transition structures by eclipsing strain. Thus, eclipsing effects in the transition states explain the stereochemistry of  $\gamma$ -lactone enolate alkylation. The energy difference between the most stable anti-transition structure **4-1a** and the most stable syn-transition structure **4-1s** is 1.00 kcal/mol, which corresponds to 93:7 selectivity at  $-78$  °C. By counting all the transition structures using the Boltzmann equation, the selectivity is 92:8 at  $-78$  °C. These calculations predict the stereochemistry of the product correctly.<sup>18</sup>

**The Origin of the Stereoselectivity of  $\gamma$ -Valerolactone Enolate.** Although Koga and Tomioka suggested that the oxygen atom in the side chain is important for the conformation of **2**, any favorable effect of the alkoxy substituent in the transition state could not be found. To see the effect of the alkoxy substituent, the stereoselectivity of the alkylation reaction of  $\gamma$ -valerolactone, which lacks alkoxy substituent in the side

chain, was studied computationally. From experimental study it had been reported that the alkylation of  $\gamma$ -valerolactone with benzyl bromide in THF by using LDA at  $-78$  °C gave 10:19<sup>a,19</sup> (83% yield) anti-stereoselectivity. The reaction of 5-*n*-tridecyl- $\gamma$ -butyrolactone with methyl iodide in THF–HMPA also gave mainly the anti-product (77% yield).<sup>9b</sup> These experimental results show that the oxygen atom in the side chain is not very important for the stereoselectivity. Although the big trityl or diphenyl *t*-butylsilyl group has some extra effect to increase the stereoselectivity, they are not necessary for this anti-selectivity. The transition state structures for the reaction of the free enolate **5** derived from  $\gamma$ -valerolactone with CH<sub>3</sub>Cl were located at the B3LYP/6-31+G\* level (Figure 3). The distances of the forming C–C bonds are 2.52 and 2.50 Å, and the activation energies are 4.63 and 5.32 kcal/mol for **anti-TS-5** and **syn-TS-5**, respectively. The transition structure **anti-TS-5** is 0.77 kcal/mol more favorable than that of **syn-TS-5**. This energy difference corresponds to the product ratio, anti:syn = 88:12 at  $-78$  °C, in good agreement with the experimental results. There is no steric interaction in these transition structures. The Newman projections from the directions indicated by arrows 1 and 2 show that **anti-TS-5** has a staggered arrangement of all the vicinal bonds at the enolate carbon

(18) The alkylation of the chiral lactones **2** with a smaller R group gave lower selectivity compared with that for **2a** (R = CPh<sub>3</sub>). For examples, anti:syn = 80:20 (R = *p*-MeOC<sub>6</sub>H<sub>4</sub>CH<sub>2</sub> with MeI),<sup>8c</sup> 92:8 (R = SO<sub>2</sub>Naphthyl, with MeI),<sup>7a</sup> and 86:14 (R = SiMe<sub>2</sub>Bu<sup>t</sup> with PhCH<sub>2</sub>Br).<sup>8c</sup>

(19) In our hand, 93:7 anti-stereoselectivity was obtained from the reaction of  $\gamma$ -valerolactone with benzyl bromide in THF (LDA,  $-78$  °C). The selectivity is slightly reduced in THF–HMPA (2 equiv) (87:13). Successive dialkylation of  $\gamma$ -valerolactone with methyl iodide and then benzyl bromide in THF (LDA,  $-78$  °C) gave 93:7 anti-selectivity.

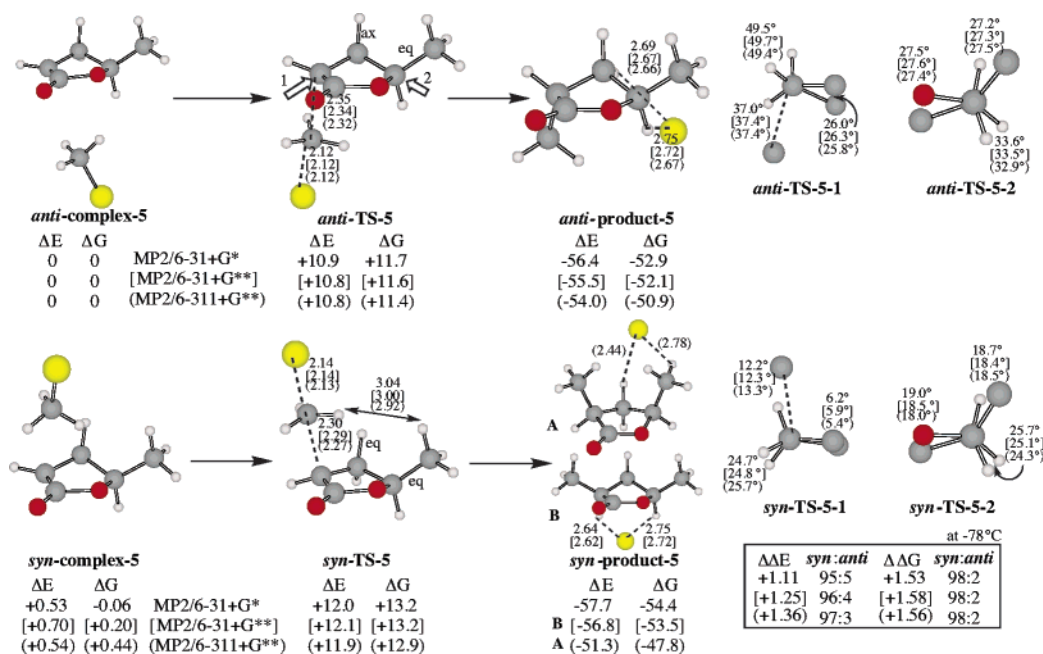


**Figure 4.** Transition structures for the anti- and syn-attacks of MeCl on the free enolate **5** (MP2/6-311+G\*\*).  $\Delta E$  and  $\Delta G$  are the differences in energy and the Gibbs free energy at  $-78^\circ\text{C}$ , respectively (kcal/mol).  $\Delta\Delta E$  and  $\Delta\Delta G$  are the syn,anti-TS energy differences. The values of MP2/6-31+G\* and [MP2/6-31+G\*\*] levels are also shown.

undergoing the hybridization change, while **syn-TS-5** has an eclipsed arrangement.

Since  $\gamma$ -valerolactone enolate has only one conformation, more detailed study of this system was performed. For comparison, the transition structures were located at the MP2/6-31+G\* level of theory (Figure 3). The distances of the forming C–C bonds at the MP2 level are much shorter than the B3LYP values (2.35 vs 2.52 and 2.30 vs 2.50 Å). The activation free energies are 11.7 and 13.3 kcal/mol for **anti-TS-5** and **syn-TS-5**, respectively, which are much higher than the B3LYP values. The results at the RHF/6-31+G\* level are also shown in Figure 3. Although the transition structures were slightly different from each other depending on the calculation levels, the syn:anti-energy differences ( $\Delta\Delta E$ ) are 1.11–1.37 kcal/mol at all levels. Furthermore, the syn:anti-energy difference computed using a higher level of correlation method, CCSD(T)/6-31+G\* with the MP2/6-31+G\* geometries, is 1.28 kcal/mol. The transition structure **anti-TS-5** is more favorable than **syn-TS-5** at all levels. The Newman projections show that **anti-TS-5** has a staggered arrangement, while **syn-TS-5** has an eclipsed one at all levels. The starting complex **anti-complex-5** has about the same stability as **syn-complex-5**. The product **syn-product-5** has a diequatorial conformation and is lower in energy than **anti-product-5**, which has one methyl equatorial and the other axial. The interaction between the  $\text{Cl}^-$  and two H's on the lower side of the ring in the products can be explained by the stabilizing electrostatic interactions. Thus, the reaction is kinetically controlled, and the main source of the anti-selectivity is an eclipsing strain in the syn-transition structure.

Basis set effects were also examined by the comparison of the MP2 results with the 6-31+G\*, 6-31+G\*\*, and 6-311+G\*\* basis sets (Figure 4). Both the structures and their energies are almost the same with one exception of the **syn-product-5** by MP2/6-311+G\*\*, in which the  $\text{Cl}^-$  interacts with the upper side H of the ring and one of the methyl protons. Although the ring inversion is easy, the  $\text{Cl}^-$  seems to fix the unstable diaxial

conformation. When the ring inversion occurs, the  $\text{Cl}^-$  moves to the lower side of the ring to interact with two H's, including the ring protons. Thus, the 6-31+G\* basis set is as good as the 6-311+G\*\* basis set for the transition structures. It even gives similar results for nonbonded interactions between the  $\text{Cl}^-$  and the protons (see the distances between the  $\text{Cl}^-$  and H's in the products).

**The Effects of a Lithium Ion and Solvent for the Alkylation Stereoselectivity.** On the basis of the small solvent effect on the stereoselectivity, free enolates were used as model systems as noted above. Here I examine the effects of a lithium ion and solvent for the alkylation stereoselectivity. The transition structures for the reaction of the lithium enolate **6** derived from  $\gamma$ -valerolactone with  $\text{CH}_3\text{Cl}$  were located at the MP2, B3LYP, and HF levels of theory with the 6-31+G\* basis set (Figure 5). The distances of the forming C–C bonds are much shorter (0.23–0.40 Å) than the values of the corresponding free enolate **5**, and the activation energies are higher than those by about 30 kcal/mol at all levels. The transition structure **anti-TS-6** is 1.01–1.06 and 1.01–1.02 kcal/mol more favorable than **syn-TS-6** in energy and Gibbs free energy, respectively. These energy differences correspond to the product ratio anti:syn = 93:7 at  $-78^\circ\text{C}$ , in good agreement with the experimental results.<sup>19</sup> The Newman projections from the directions indicated by arrows 1 and 2 show that **anti-TS-6** has a staggered arrangement, while **syn-TS-6** has an eclipsed arrangement. Although a small steric repulsion is detected between the incoming methyl group and the side chain methyl in **syn-TS-6** at both the MP2 and the B3LYP levels, the main source of the anti-selectivity is an eclipsing strain in the syn-transition structure.

The product **syn-product-6** has a diaxial conformation **C** at the MP2 level and a diequatorial conformation **D** at both the B3LYP and the HF levels. The position of LiCl is also very different in **anti-product-6** depending on the calculation level. These conformation changes in the products come from the

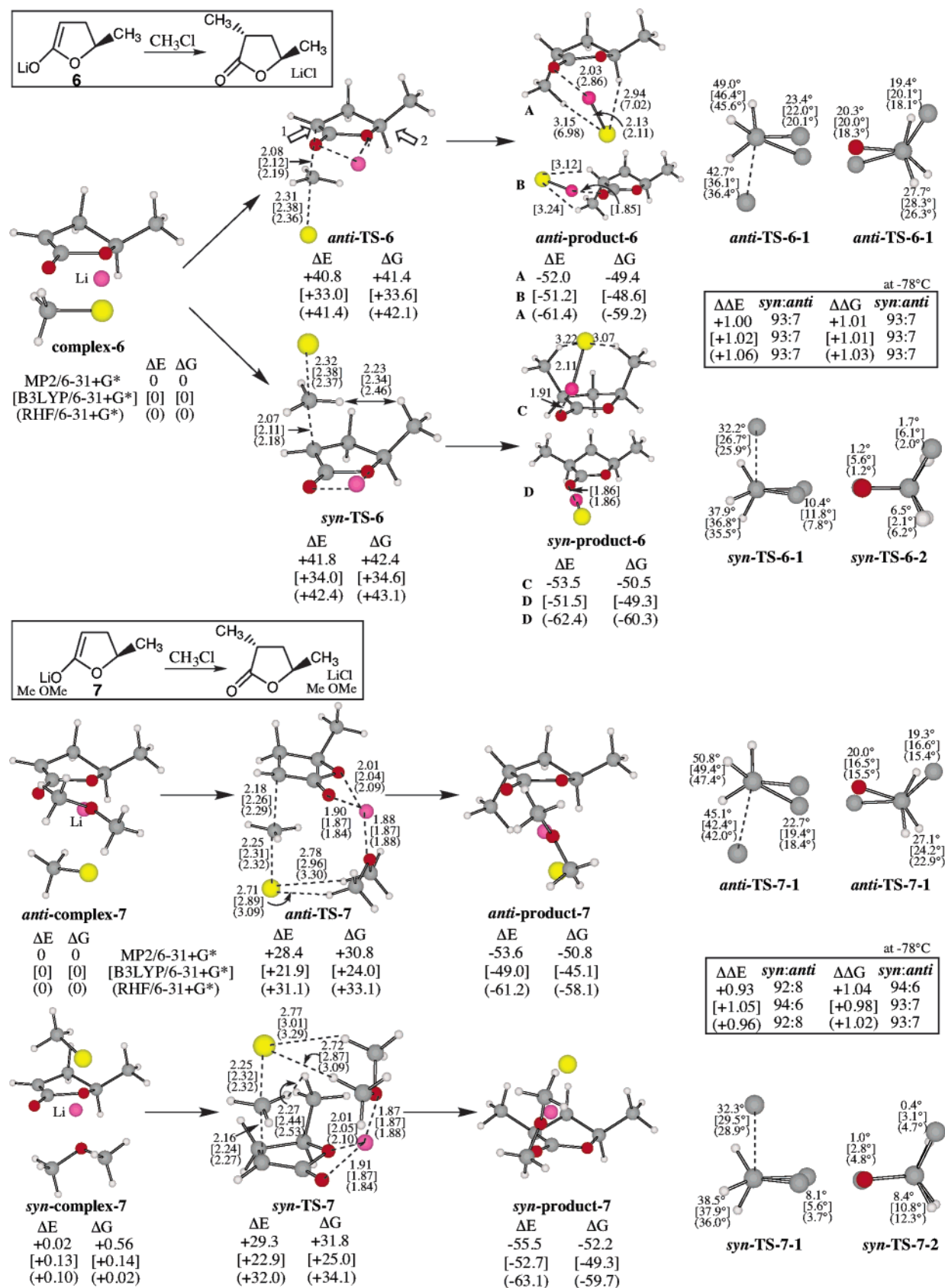


**Figure 5.** Transition structures for the anti- and syn-attacks of MeCl on the lithium enolate **6** and **7** (MP2/6-31+G\*).  $\Delta E$  and  $\Delta G$  are the differences in energy and the Gibbs free energy at -78 °C, respectively (kcal/mol).  $\Delta\Delta E$  and  $\Delta\Delta G$  are the *syn,anti*-TS energy differences. The values of [B3LYP/6-31+G\*] and (RHF/6-31+G\*) are also shown.

different treatment of the weak nonbonded interactions depending on the calculation level.

Since the alkylation reaction of these lactones was generally performed in THF, solvation of the lithium ion is expected to

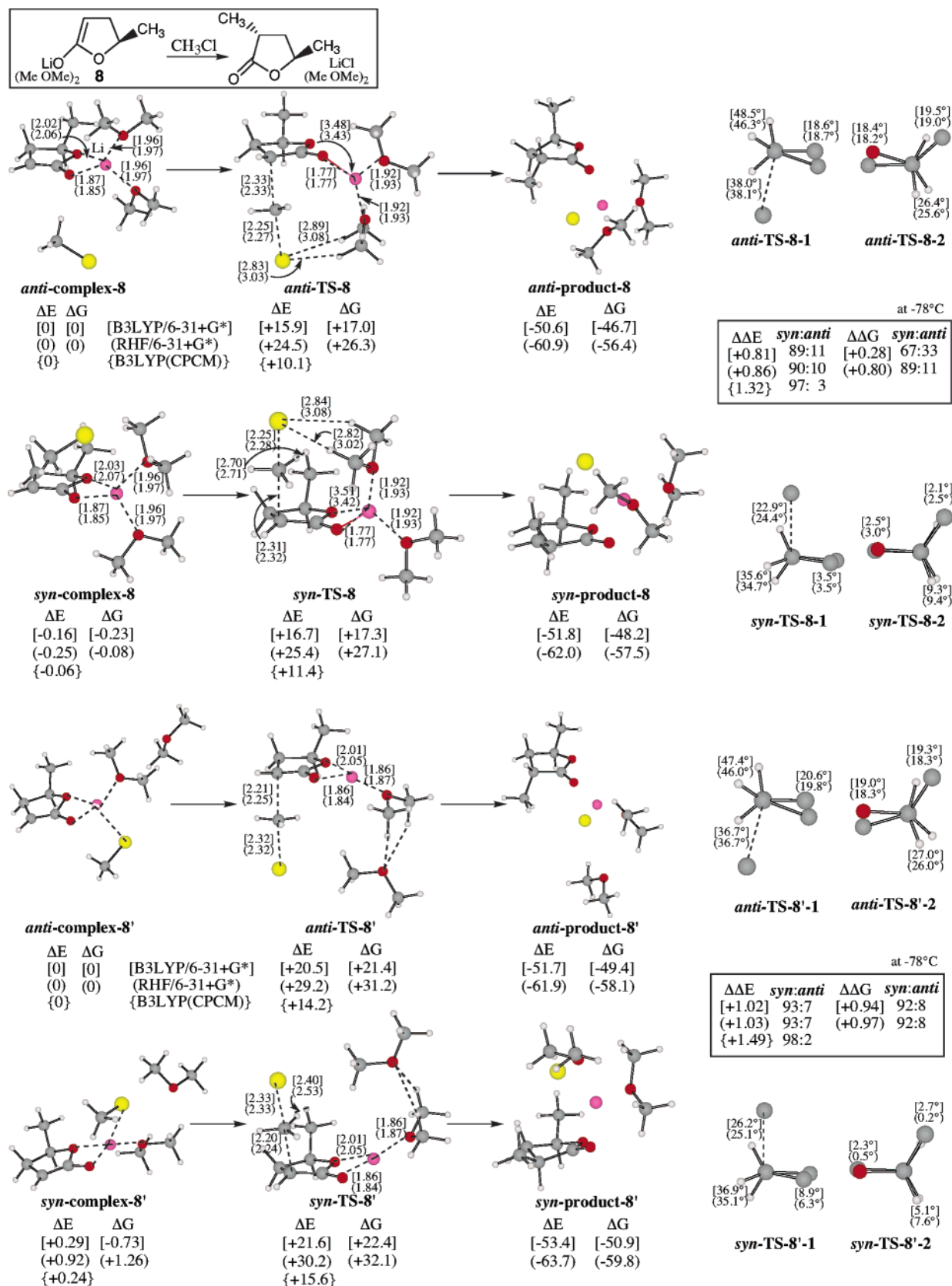


**Figure 6.** Transition structures for the anti- and syn-attacks of MeCl on the lithium enolate **8** and **8'** [B3LYP/6-31+G\*].  $\Delta E$  and  $\Delta G$  are the differences in energy and the Gibbs free energy at  $-78^\circ\text{C}$ , respectively (kcal/mol).  $\Delta\Delta E$  and  $\Delta\Delta G$  are the syn,anti-TS energy differences. The values of (RHF/6-31+G\*) and {B3LYP/6-31+G\* SCRF(CPCM, solvent = THF)}/B3LYP/6-31+G\* levels are also shown.

be important. Such solvation was approximated as the coordination of ether oxygen to the lithium ion. Dimethyl ether has about the same basicity and steric effect as THF but significantly

smaller for computations.<sup>20</sup> Therefore, dimethyl ether was chosen as the coordinating solvent. The transition structures for the reaction of the lithium enolate **7** coordinated with one



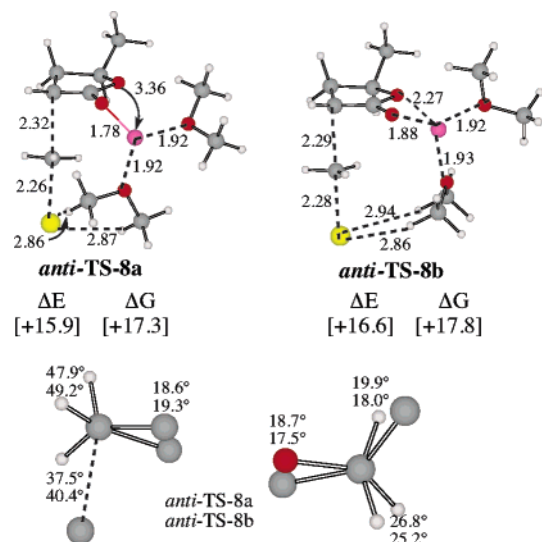


Figure 7. B3LYP/6-31+G\*.

dimethyl ether molecule with  $\text{CH}_3\text{Cl}$  were located at the MP2, B3LYP, and HF levels of theory with the 6-31+G\* basis set (Figure 5). The coordination of the dimethyl ether molecule made the distances of the forming C–C bonds longer by 0.09–0.14 Å and the activation energies much reduced (12.52–10.30 kcal/mol less in energy and 10.57–8.94 kcal/mol less in Gibbs free energy) at all levels compared with the results from **6**. The interaction between the leaving chloride atom and the ether protons can be explained by the electrostatic interactions.

The transition structure **anti-TS-7** is 0.93–1.05 and 0.98–1.04 kcal/mol more favorable than **syn-TS-7** in energy and Gibbs free energy, respectively. These energy differences correspond to the product ratio, anti:syn = 92:8 to 94:6 at  $-78^\circ\text{C}$ , in good agreement with the experimental results. The Newman projections from the directions indicated by the arrows 1 and 2 show that **anti-TS-7** has a staggered arrangement, while **syn-TS-7** has an eclipsed arrangement. Although a small steric repulsion is detected between the incoming methyl group and the side chain methyl in **syn-TS-7** at the MP2 level, the main source of the anti-selectivity is an eclipsing strain in the syn-transition structure.

The transition structures for the reaction of the lithium enolate **8** coordinated with two ether molecules with  $\text{CH}_3\text{Cl}$  were located at the B3LYP/6-31+G\* level. Three kinds of anti-transition structures (**anti-TS-8**, **anti-TS-8a**, and **anti-TS-8b** in Figures 6 and 7) were obtained. Although **anti-TS-8b** has a tetracoordinated lithium ion, tricoordinated structures **anti-TS-8** and **anti-TS-8a** are more favorable than that. For monodentate ethers, coordination is accompanied by substantial loss of entropy. In many cases, tricoordinated lithium compounds are the most important.<sup>20,21</sup> Since the arrangement of ether molecules in **anti-TS-8** is the same as the one in **syn-TS-8**, the most stable transition structure **anti-TS-8** was compared with **syn-TS-8** in Figure 6. The results at the RHF/6-31+G\* level are also shown in Figure 6. The distances of the forming C–C bonds lengthen by the coordination of two ether molecules by 0.04–0.07 Å, and the activation energies are lower by about 7 kcal/mol at all

levels compared with the results from **7**. The transition structure **anti-TS-8** is 0.81–0.86 and 0.28–0.80 kcal/mol more favorable than **syn-TS-8** in energy and Gibbs free energy, respectively. A small Gibbs free energy difference (0.28 kcal/mol) was obtained at the B3LYP level. Since the ether molecules have an interaction both with the lithium atom and the leaving chloride atom, substantial loss of entropy is expected. Therefore, we further located the transition structures for the reaction of the lithium enolate **8'** with the coordination of one ether oxygen atom to the lithium ion and the other ether to the chloride atom (the bottom of Figure 6). The transition structure **anti-TS-8'** is 1.02–1.03 and 0.94–0.98 kcal/mol more favorable than **syn-TS-8'** in energy and Gibbs free energy, respectively. These energy differences correspond to the product ratio, anti:syn = 92:8 to 93:7 at  $-78^\circ\text{C}$ , in good agreement with the experimental results. The Newman projections show that **anti-TS-8** and **anti-TS-8'** have a staggered arrangement, while **syn-TS-8** and **syn-TS-8'** have an eclipsed arrangement. Since there is no steric interaction in these transition structures, the main source of the anti-selectivity is an eclipsing strain in the syn-transition structure.

Furthermore, the self-consistent reaction field (SCRF) technique for THF ( $\epsilon = 7.58$ ) was used to examine the bulk of solvent effects except for the special interactions between the substrate and the solvent. The energies of **anti,syn-TS-8** and **8'** and **anti,syn-complex-8** and **8'** were calculated at the B3LYP/6-31+G\* level with Tomasi's polarized continuum model using the polarizable conductor calculation model [SCRF-(CPCM, solvent = THF)].<sup>22</sup> The activation energies were reduced by 5.28–6.29 kcal/mol, and the energy differences between the anti- and syn-transition structures are slightly increased as shown in Figure 6.

## Conclusion

Conformer search of the free enolate generated from 4-methoxymethyl- $\gamma$ -butyrolactone gave 15 unique conformers within 5.39 kcal/mol at the B3LYP/6-31+G\* level. The transition structures for both anti- and syn-attack of methyl chloride on these 15 conformers were located. In all cases, the anti-transition structures are more stable than the corresponding syn-ones. In the anti-transition structures, the incoming methyl group from the axial direction makes the anti-hydrogen on the next carbon axial. Since the  $\text{MeOCH}_2$  group prefers to be equatorial, this arrangement makes transition structure more staggered. On the other hand, the incoming methyl group in the syn-transition structures makes the *syn*-H on the next carbon equatorial. Since the  $\text{MeOCH}_2$  group prefers to be equatorial, the lactone ring becomes flatter. Thus, the eclipsing effects in the syn-transition structures control the stereoselectivity of this alkylation reaction. To see the effect of the alkoxy substituent, the stereoselectivity of the alkylation reaction of  $\gamma$ -valerolactone, which lacks methoxy group in the side chain, was studied. The transition structures for the alkylation of the free enolate, the lithium enolate, and the lithium enolate solvated with dimethyl ether were located at MP2, B3LYP, and HF levels of theory with the 6-31+G\* basis set. The anti-transition structures are more favorable than the corresponding syn-transition structures at all levels of theory in every model. Although the presence of the

(20) (a) Abbotto, A.; Streitwieser, A.; Schleyer P. v. R. *J. Am. Chem. Soc.* **1997**, *119*, 11255–11268. (b) Pratt, L. M.; Streitwieser, A. *J. Org. Chem.* **2003**, *68*, 2830–2838.

(21) Ando, K. *J. Org. Chem.* **1999**, *64*, 6815–6821.

(22) Barone, V.; Cossi, M. *J. Phys. Chem. A* **1998**, *102*, 1995–2001.

lithium ion and solvent change the length of the forming C–C bond in the transition structures, the Newman projections are similar in all models and calculation levels. The anti-transition structures have a staggered arrangement, while the syn-transition structures have an eclipsed arrangement. The energy differences between the anti- and syn-transition structures are about 1 kcal/mol and in good agreement with the experimental data. This study shows that there is no special effect of the alkoxy substituent and that the main source of the anti-selectivity of 4-alkoxymethyl- $\gamma$ -butyrolactone is eclipsing strain in the syn-transition structures.

**Acknowledgment.** This work was partially supported by The Japan Securities Scholarship Foundation. I thank the Computer Center of the Institute for Molecular Science, Okazaki, Japan for the use of VPP5000 computer. This article is dedicated to the memory of Professor Kenji Koga.

**Supporting Information Available:** Figure and the *xyz* coordinates for the transition structures **4–1a,s** and **4–2a,s** and the MP2/6-31+G\* structures *anti,syn-TS-5*, *anti,syn-TS-6*, and *anti,syn-TS-7*. This material is available free of charge via the Internet at <http://pubs.acs.org>.

JA044995N